



Published  
for the  
International  
Glaciological  
Society

THIS MANUSCRIPT HAS BEEN SUBMITTED TO THE JOURNAL OF GLACIOLOGY AND HAS NOT BEEN PEER-REVIEWED.

### Tracking glacier surge evolution using interferometric SAR coherence – examples from Svalbard

Journal:	<i>Journal of Glaciology</i>
Manuscript ID	JOG-2024-0133
Manuscript Type:	Letter
Date Submitted by the Author:	10-Oct-2024
Complete List of Authors:	Schytt Mannerfelt, Erik; University of Oslo Department of Geosciences; University Centre in Svalbard, Arctic Geology Schellenberger, Thomas; University of Oslo Department of Geosciences Kaab, Andreas; University of Oslo Department of Geosciences
Keywords:	Glacier surges, Remote sensing, Ice dynamics
Abstract:	We present a practically simple methodology for tracking glacier surge onset and evolution using interferometric Synthetic Aperture Radar (InSAR) coherence. Detecting surges early and monitoring their build-up is interesting for a multitude of scientific and safety-related aspects. We show that InSAR coherence maps allow the detection of surge-related instability on Svalbard many years before being detectable by, for instance, feature tracking or crevasse detection. Furthermore, we present derived data for two types of surges; downstream- and upstream-propagating, with interestingly consistent surge propagation and post-surge relaxation rates. The method works well on Svalbard glaciers, and the data and core principle suggest a global applicability.

SCHOLARONE™  
Manuscripts

# Tracking glacier surge evolution using interferometric SAR coherence — examples from Svalbard

Erik Schytt MANNERFELT,<sup>1,2</sup> Thomas SCHELLENBERGER,<sup>1</sup> Andreas M. KÄÄB<sup>1</sup>

<sup>1</sup>*Department of Geosciences, University of Oslo, Oslo, Norway*

<sup>2</sup>*Arctic Geology, The University Centre in Svalbard, Norway*

*Correspondence: <e.s.mannerfelt@geo.uio.no>*

**ABSTRACT.** We present a practically simple methodology for tracking glacier surge onset and evolution using interferometric Synthetic Aperture Radar (InSAR) coherence. Detecting surges early and monitoring their build-up is interesting for a multitude of scientific and safety-related aspects. We show that InSAR coherence maps allow the detection of surge-related instability on Svalbard many years before being detectable by, for instance, feature tracking or crevasse detection. Furthermore, we present derived data for two types of surges; downstream- and upstream-propagating, with interestingly consistent surge propagation and post-surge relaxation rates. The method works well on Svalbard glaciers, and the data and core principle suggest a global applicability.

## INTRODUCTION

Glacier surges are sudden temporary glacier speed-ups, sometimes by one or many orders of magnitudes. They pose local safety hazards by damming lakes that subsequently outburst (Post and Mayo, 1971; Bazai and others, 2021), or for travel across glaciers, and reveal problems in our understanding of general glacier dynamics due to our inability to properly predict them beforehand. Work has been done on glaciers that are on the brink of surging (e.g. Clarke, 1976; Bouchayer and others, 2024), but the lack of indications before surges means they are generally not known before it is too late to study their evolution in situ. Here, we present a new tool for detecting glacier surges years before they become detectable by established methods, and present statistics on the rates of surge progression for glaciers on Svalbard.

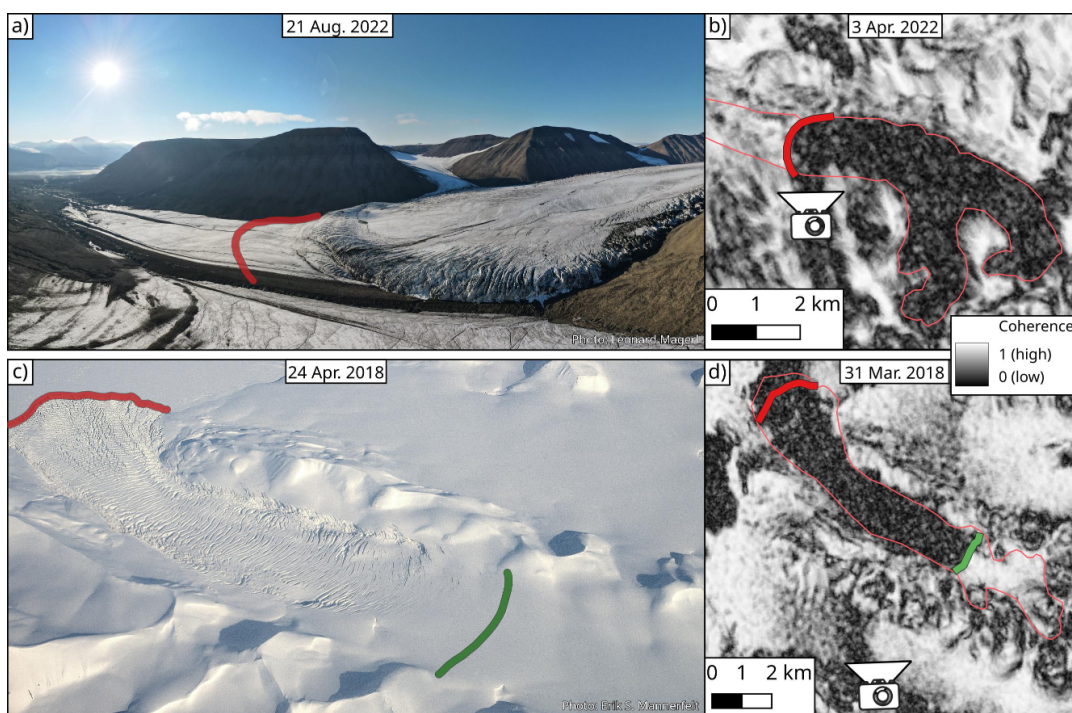


**Fig. 1.** In-situ photographs compared to coherence maps in the same year. **a)** Bulge-initiated surge of Val-låkrabreen, showing a surge bulge with splaying crevasses and a less pronounced forebulge ahead of it. The red line shows the approximate location of the low-coherence boundary from earlier that year (shown in **b**, together with the photo location); roughly coincident with the forebulge. **c)** terminus initiated surge of Arnesenbreen, showing the lower surge boundary in red and the upper low-coherence boundary in green (c.f. panel **d**). We presume that the discrepancy between the green line in **c**) and the region of substantial crevassing is due to coherence being sensitive to smaller disturbances than what can be seen in a winter photograph. The largest surge extent (so far) is shown in pink outlines for panels **b**) and **d**).

26 Previous methods of surge detection involve identifying sudden changes in geometry, texture or surface  
 27 velocity of a glacier. Elevation change maps reveal large mass displacement events (e.g. Paul and others,  
 28 2022). If the surface velocity is high enough, i.e. when a surge has accelerated sufficiently, it can also  
 29 be autonomously detected using feature tracking (surface velocity) time series (Koch and others, 2023).  
 30 Drastic increases in crevassing is finally a robust method of identifying an ongoing surge through subtracting  
 31 SAR backscatter intensity images over time (Kääb and others, 2023). While all of these methods work  
 32 well on their own, they mostly function when the glacier is already fully surging; characterising the build-  
 33 up is much more difficult. High-accuracy elevation data can technically be used over long time periods to  
 34 reveal unstable mass redistribution associated with future surging (Sund and others, 2009). Acquiring these  
 35 elevation data at high accuracy and temporal frequency requires thorough processing and error assessment,  
 36 however (c.f. Hugonnet and others, 2022); finding an easier and less resource-intensive method would clearly  
 37 be advantageous.

38 Repeated Synthetic Aperture Radar (SAR) acquisitions of terrain can be used to assess changes in  
39 signal phase, affected by terrain motion and changes in reflective characteristics. Interferometric SAR  
40 (InSAR), the process of describing these phase changes, is commonly used in cryospheric sciences, e.g. for  
41 ground subsidence (Rouyet and others, 2021), glacier velocity (Eldhuset and others, 2003) and classification  
42 of debris covered glaciers (Thomas and others, 2023). While normal InSAR workflows generally involve  
43 heavy post-processing to obtain displacement products, a simpler and useful by-product is the normalized  
44 cross-correlation of two single-look complex (SLC) SAR scenes, usually denoted as coherence. InSAR  
45 coherence varies in the range of 0 (no phase correlation between two acquisitions) to 1 (the phase between  
46 acquisitions is identical), and is normally used for quality assessment of the co-registration (Eldhuset and  
47 others, 2003), masking out low-coherence areas within phase unwrapping, and terrain classification (Shi  
48 and others, 2019), including mapping of debris-covered parts of glaciers that are difficult to do using  
49 optical methods (Atwood and others, 2010; Frey and others, 2012). Coherence is normally lost either  
50 if terrain displacement or nonlinear motion components (shear, rotation, etc.) become too large, or if  
51 terrain reflective characteristics change, for example during a rainfall event or during ice- or snowmelt  
52 (Weydahl, 2001). Thus, in intervals featuring stable cold weather, the presence or absence of significant  
53 glacier motion, motion gradients, and deformation can be assessed visually or computationally using InSAR  
54 coherence maps.

55 Many or most glaciers on Svalbard have a recent past of surging (Sevestre and Benn, 2015; Farnsworth  
56 and others, 2016), meaning most currently non-surging glaciers can be described as being in quiescence.  
57 Quiescent glacier surface velocities are usually low, measuring 5–18 m / yr on Svalbard (Nuttall and others,  
58 1997; Sund and Eiken, 2004; Sund and others, 2014). Surges dramatically increase this speed to a few or  
59 tens of metres per day instead, and this order-of-magnitude change can be used for detection. Two types of  
60 surge propagation directions have been shown to exist on Svalbard; downstream propagating, characterised  
61 by a surface bulge (e.g. Murray and others, 1998), or upstream propagating, i.e. in a terminus initiated  
62 surge (Sevestre and others, 2018). In Alaska, synchronous up- and downstream propagation of a surge  
63 that initiates in the central body has been shown (Altena and others, 2019), but this has not yet been  
64 described on Svalbard. Improved monitoring of surge propagation would thus certainly contribute to better  
65 characterising and understanding of the (potentially different) types of surge evolution and its direction  
66 with respect to the direction of glacier flow.

67 We demonstrate the usefulness InSAR coherence maps on Svalbard for tracking down- or upstream

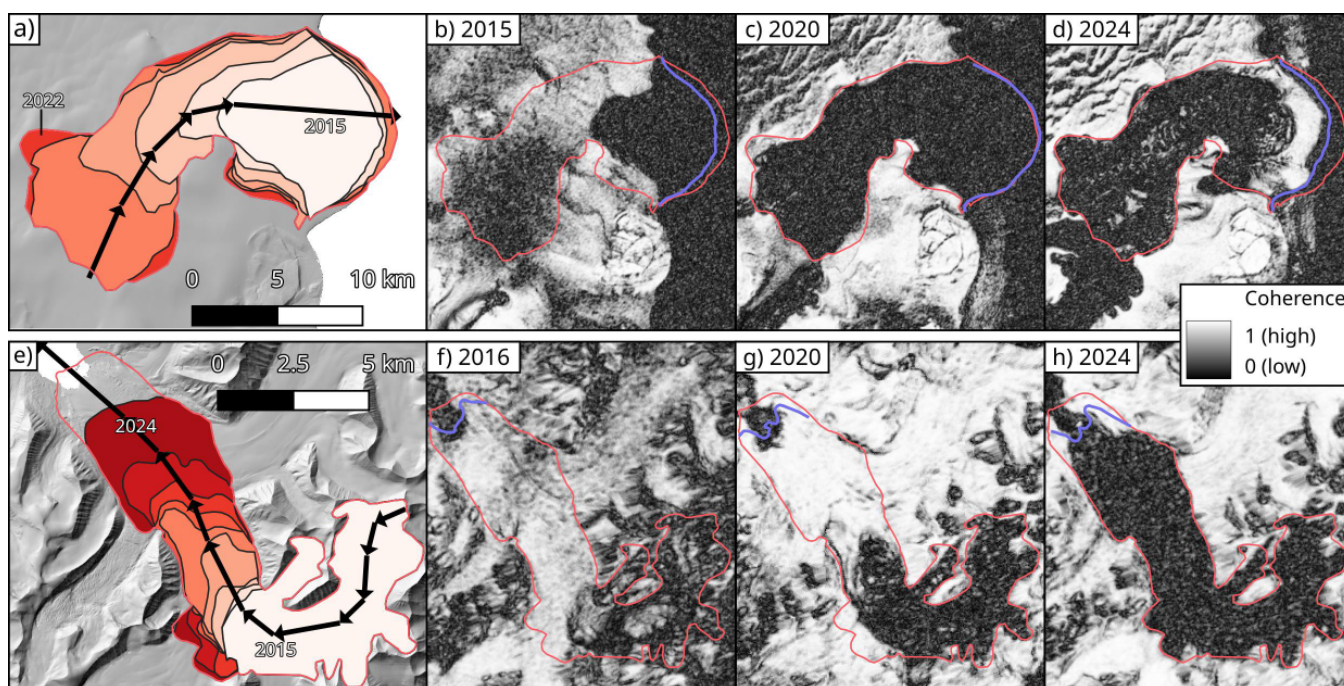


**Fig. 2.** Examples of coherence changes during the progression of two surges. **Top (a–d):** Terminus-initiated surge of Stonebreen. Note the onset of stagnation in 2024 (d) shown by the terminus regaining coherence. **Bottom (e–h):** Surge bulge propagation of Paulabreen. The pink outlines in all panels represent the maximum attained extent of the surges so far, and the blue lines represent the concomitant front positions. Basemap hillshade from 2010 of panels a) and e) courtesy of the Norwegian Polar Institute.

68 propagating surges by mapping out zones of low coherence (disturbed flow) and measuring temporal changes  
 69 in their extent. Our resultant patterns show that the technique opens new doors to ways of quantifying  
 70 surging, and allows for rough empirical predictions of the timing of surge acceleration. While our study  
 71 focuses on Svalbard only, the data and techniques can be used for global assessments of surge propagation  
 72 rates and patterns in regions with similarly low quiescent baseline flow.

## 73 DATA AND METHODS

74 We obtain processed Sentinel-1 inSAR coherence maps from the Alaska Satellite Facility (ASF) Vertex tool  
 75 (<https://search.asf.alaska.edu>). We order the processing of every 12-day acquisition pair since the  
 76 beginning of the Sentinel-1 record on Svalbard (January 2015) in the winter months of 1 November to 30  
 77 April. We choose this interval as spring or summer melt strongly reduces the phase coherence and renders  
 78 the data unusable for our purposes. Qualitative assessments of 6-day returns using the Sentinel-1A and  
 79 -B satellites revealed much cleaner coherence maps, but we stayed consistent with 12-day baselines as the  
 80 6-day availability period lasted only a subset of the study period (Oct. 2016 to Dec. 2021) due to the failure

81 of Sentinel-1B. A total of 797 scenes were successfully processed, with some failures due to co-registration  
82 errors not converging below the pre-set threshold. Most 12-day pairs show very low coherence throughout  
83 the scene due to weather effects (Weydahl, 2001). We sift through the entire catalogue manually for each  
84 glacier, and extract at least one suitable coherence map per year. For each good scene, we manually  
85 delineate any encountered low-coherence front with an upper and/or lower boundary line. A detailed  
86 investigation of the influence and the spatio-temporal variations of factors that contribute to coherence  
87 loss at the surge fronts (in particular likely motion magnitude, motion gradients, surface deformation, and  
88 surface changes by crevasse formation) is out of scope for this brief communication and remains to be done.  
89 However, comparison of our coherence-derived surge fronts to in-situ photographs (Figure 1) and DEM  
90 differences between occasional individual ArcticDEM products shows that our coherence-derived surge  
91 fronts coincide with topographic bulges, thus indicating a change in glacier mass transport. To obtain  
92 terminus positions, we download Sentinel-1 backscatter intensity and Sentinel-2 L1C true colour scenes  
93 for manual terminus delineation. We assess length and length change along a manually drawn glacier  
94 centreline, measuring the glacier terminus, the lower and upper low-coherence front. We measure lengths  
95 of buffered centrelines within  $\pm 200$  m of the discrete centreline to obtain a spread and to reduce uncertainty  
96 in the exact placement of the centreline. The chosen buffer width of  $\pm 200$  m is open to discussion, but not  
97 critical for this method demonstration study.

98 In order to derive further statistics of the mapped surges, we divide them in three stages (if observed);  
99 pre-surge, surge, and post-surge, based on our available data. The surge date is defined differently for down-  
100 and upstream propagating surges. For downstream propagating surges, we simply assign the date when  
101 the low-coherence front (surge bulge) reaches the terminus. For upstream propagating surges, we choose a  
102 low-coherence expanse threshold whereafter the glacier typically starts to advance. As tidewater glaciers  
103 often naturally advance in winter due to sea ice lowering the calving rate, we could not use a simple advance  
104 rate threshold. We observe that all mapped upstream-propagated surging glaciers advanced, regardless of  
105 season, when 40% or more of the glacier had lost coherence (Supplementary Figure S1). Thus, we use  
106 this 40% coverage threshold to define the start of an upstream propagating surge. An exception is made  
107 at the glacier Etonbreen as it is part of an ice cap and therefore has an undefined upper bound. Instead,  
108 we used the date when the glacier first advanced without the help of a sea-ice buffer (November 2023).  
109 The surge termination is defined the same for both types of surges; when the terminus regains coherence  
110 and thus shows a near or total stagnation at the front. We want to highlight that the exact definition of

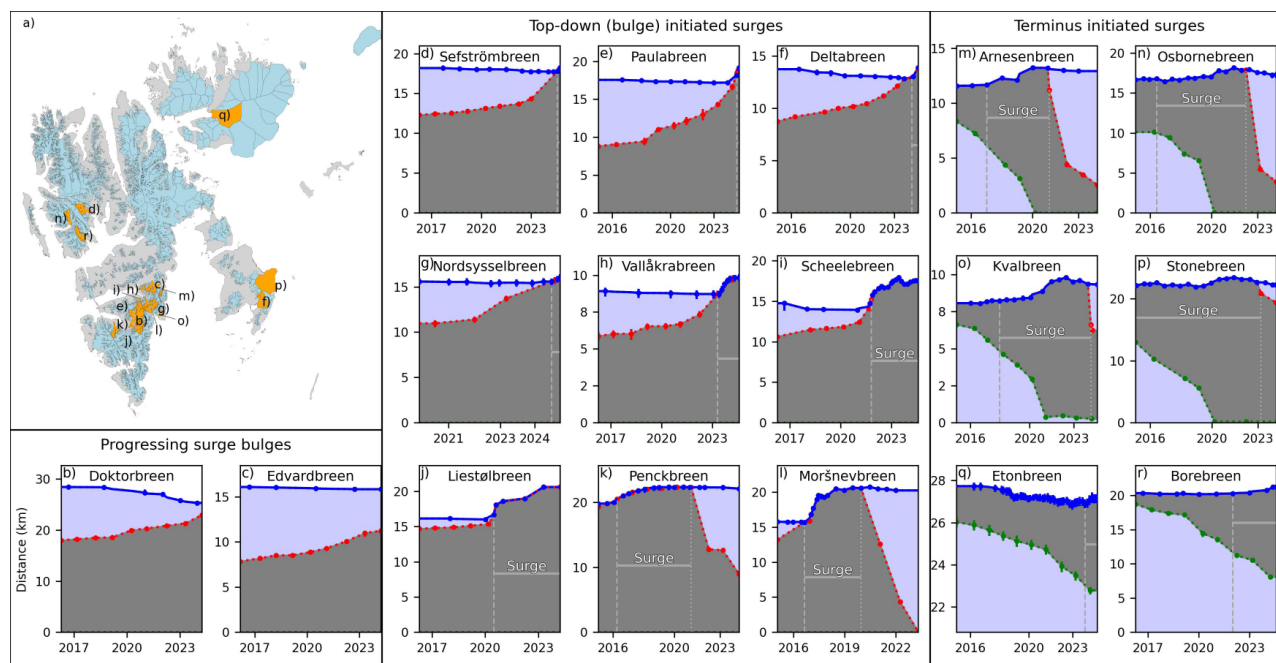


**Fig. 3.** Digitised low-coherence (surge) front progressions for surges on Svalbard. **a)** Overview map showing all glaciers (blue) and the location of the presented glaciers (orange plus letters). Glacier front outlines are from Nuth and others (2013). **b–c)** Low-coherence front progressions that indicate a future advance. **d–l)** Top-down (bulge) propagating surge examples. **m–r)** Bottom-up (terminus initiated) surge examples. High-coherence parts of the glacier are shaded light blue, low-coherence parts are shaded grey, front positions are shown in blue, the lower boundary of the low-coherence front in red, and the upper boundary in green. Points (with 25th to 75th percentile spreads) represent measured values, and the parts in between are interpolated. For reference, **c)** is lake-terminating, **h), i)** (before 2022) and **k)** are land-terminating, and the rest are tidewater glaciers.

111 when a surge starts and ends, where it does so, and which indicators are used to define them are all up to  
 112 discussion; we rather see our dates as common "milestone" events along the continuum of surge behaviour.

## 113 RESULTS

114 We present statistics from 18 recently terminated or still ongoing surging glaciers on Svalbard. Out of these,  
 115 12 initiated by propagating downstream and 6 by propagating upstream. We focus on aggregate statistics  
 116 here; individual glacier information is found in the Supplementary Table S1. Unless otherwise specified,  
 117 the presented numbers show the median $\pm$ standard deviation. We find that downstream propagating surges  
 118 generally lead to significantly faster terminus advance rates ( $4.69\pm 6.00$  m/d) compared to the upstream  
 119 propagating counterparts ( $0.51\pm 0.44$  m/d). However, the instability propagation itself generally shows  
 120 an opposite tendency, with upstream propagation rates of  $4.23\pm 1.83$  m/d and downstream propagation  
 121 rates of  $2.24\pm 2.30$  m/d. We qualitatively note an accelerating tendency of both up- and downstream  
 122 propagation rates near the beginning of the phase when the terminus advances (Figure 3). There is only a



123 weak correlation between instability propagation rates and subsequent advance rates in our data, showing  
124 Pearson correlation coefficients of 0.45 and -0.30 for down- and upstream propagating surges, respectively.  
125 In other words, there seems to be no simple way to predict the magnitude of a surge before it accelerates  
126 from these data alone.

127 The most consistent measured rate is the gradual return to coherence after a surge. Figure 2d demon-  
128 strates the ongoing stagnation of the recent Stonebreen surge, shown by regained high coherence at the  
129 terminus. All stagnating glaciers in this study show the same pattern of starting at the terminus and grad-  
130 ually continuing up-glacier. This occurs at a rate of  $12.21 \pm 3.98$  m/d, with little to no variability between  
131 down- and upstream propagated surges.

## 132 DISCUSSION

133 The identified and described surges in this study display a perhaps surprising similarity in rates and  
134 patterns of propagation, advance and subsequent stagnation. Most downstream propagating surges have  
135 a well-defined boundary between low and high coherence, with only a few edge cases where shear margins  
136 (stripes of low coherence) are seen instead (Figure 2). But the similarities should not instil overconfidence  
137 in the method, as we abandoned the characterisation of the recent surges of Monacobreen (Banerjee and  
138 others, 2022) and Tunabreen (Vallot and others, 2019); both glaciers are fast-flowing even during quiescence,  
139 featuring low glacier-wide coherence, and surge propagation monitoring is therefore not possible with our  
140 method alone.

141 An outstanding question in this work is how the initial formation of a downstream propagating insta-  
142 bility looks like. In other words, how far back in time can we detect a future downstream propagating  
143 surge? We only have vague indications of initial bulge formation; low-coherence lines associated with shear  
144 margins gradually lose coherence and subsequently start progressing down-glacier. This is exemplified at  
145 the surge of Paulabreen in Figure 2, where the 2016 scene displays only partial loss of coherence in the  
146 surge front, while the latter scenes show a total loss. This type of proto-bulge can be seen in other exam-  
147 ples throughout Svalbard (Supplementary Figure S2), and might represent the earliest detectable stage of  
148 unstable flow through this method. While interpretations turn vague too far back in time, we still see that  
149 many surges can be seen up to (and maybe longer than) eight years before they reach the front. Thus,  
150 mapping the progression of low-coherence zones on glaciers can be used as an early warning system for  
151 many surges.

152 We do not mean to convey that all cases of lost coherence mean that a surge is about to happen.  
153 Persistent low-coherence zones that could be misclassified as surge bulges are found all over Svalbard, and  
154 are most easily explained through uneven variations in subglacial topography leading to disturbed flow. In  
155 addition, all tidewater glaciers seem to feature a low-coherence zone near their termini, easily explainable by  
156 tidal effects at their calving bays. What sets out a potential surge from both of these cases in the coherence  
157 is the temporal progression; an expanding disturbance or an accelerating large terminal low-coherence zone  
158 indicates a state change in the glacier's local flow characteristics. Therefore, we are confident that all our  
159 presented examples represent actual surges, but we may have missed smaller instability progressions that  
160 got lost between all other more natural zones of low to no coherence.

## 161 CONCLUSION

162 Here, we present InSAR coherence maps as a new tool to track glacier surge evolution from its buildup  
163 phase to stagnation. While the method is only proven to work on glaciers with low baseline quiescent  
164 velocities, the ones we study show clear similarities in surge evolution rates. There is a strong case for  
165 future automation of the tool to detect surge-like glacier flow instabilities, as the ones mapped in this study  
166 are clearly visible in the coherence data with the naked eye. We could infer glacier surges many years (in one  
167 case up to eight) before they reached the front, supporting the potential use of the method for safety-related  
168 or scientific forecasting of surge-like behaviour. We believe that the method can provide new insights into  
169 the physics and evolution of glacier surges, for instance regarding the spatio-temporal patterns of initial  
170 ice-flow change. For example, our (limited) study for Svalbard suggests that the instability propagation  
171 during the build-up phase has no direct correlation with the magnitude of a later surge, meaning the  
172 physics that drive them might be different. As another potentially important result, we want to highlight  
173 that the instability propagation that eventually led to surging started many years before accelerating and  
174 advancing. This has implications for studies that investigate connections between meteorological or climatic  
175 conditions and glacier surging, as a substantial time delay between build-up conditions and the subsequent  
176 surge might have to be considered. We thus suggest that this simple method is implemented in the toolbox  
177 for detecting, mapping, classifying and tracking surges and other surge-like glacier flow instabilities.

## 178 DATA AVAILABILITY

179 The source code for InSAR post-processing and figures are found at [https://github.com/erikmannerfelt/](https://github.com/erikmannerfelt/IncoherentSurges)  
180 `IncoherentSurges`. Before the potential acceptance and publication of this manuscript, an associated Zen-  
181 do publication will be made and linked here with supporting output data.

## 182 ACKNOWLEDGEMENTS

183 TS was financed by the Research Council of Norway (“Researcher Project for Scientific Renewal”, MAS-  
184 SIVE, Project 315971)

## 185 REFERENCES

- 186 Altena B, Scambos T, Fahnestock M and Kääb A (2019) Extracting recent short-term glacier velocity evolution over  
187 southern Alaska and the Yukon from a large collection of Landsat data. *The Cryosphere*, **13**(3), 795–814, ISSN  
188 1994-0424 (doi: 10.5194/tc-13-795-2019)
- 189 Atwood DK, Meyer F and Arendt A (2010) Using L-band SAR coherence to delineate glacier extent. *Canadian*  
190 *Journal of Remote Sensing*, **36**(sup1), S186–S195, ISSN 0703-8992, 1712-7971 (doi: 10.5589/m10-014)
- 191 Banerjee D, Garg V and Thakur PK (2022) Geospatial investigation on transitional (quiescence to surge initiation)  
192 phase dynamics of Monacobreen tidewater glacier, Svalbard. *Advances in Space Research*, **69**(4), 1813–1839, ISSN  
193 02731177 (doi: 10.1016/j.asr.2021.08.020)
- 194 Bazai NA, Cui P, Carling PA, Wang H, Hassan J, Liu D, Zhang G and Jin W (2021) Increasing glacial lake outburst  
195 flood hazard in response to surge glaciers in the Karakoram. *Earth-Science Reviews*, **212**, 103432, ISSN 00128252  
196 (doi: 10.1016/j.earscirev.2020.103432)
- 197 Bouchayer C, Nanni U, Lefeuvre PM, Hult J, Steffensen Schmidt L, Kohler J, Renard F and Schuler TV (2024)  
198 Multi-scale variations of subglacial hydro-mechanical conditions at Kongsvegen glacier, Svalbard. *The Cryosphere*,  
199 **18**(6), 2939–2968, ISSN 1994-0424 (doi: 10.5194/tc-18-2939-2024)
- 200 Clarke GK (1976) Thermal Regulation of Glacier Surging. *Journal of Glaciology*, **16**(74), 231–250, ISSN 0022-1430,  
201 1727-5652 (doi: 10.3189/S0022143000031567)
- 202 Eldhuset K, Andersen PH, Hauge S, Isaksson E and Weydahl DJ (2003) ERS tandem InSAR processing for DEM  
203 generation, glacier motion estimation and coherence analysis on Svalbard. *International Journal of Remote Sensing*,  
204 **24**(7), 1415–1437, ISSN 0143-1161, 1366-5901 (doi: 10.1080/01431160210153039)

- 205 Farnsworth WR, Ingólfsson O, Retelle M and Schomacker A (2016) Over 400 previously undocumented Svalbard  
206 surge-type glaciers identified. *Geomorphology*, **264**, 52–60, ISSN 0169555X (doi: 10.1016/j.geomorph.2016.03.025)
- 207 Frey H, Paul F and Strozzi T (2012) Compilation of a glacier inventory for the western Himalayas from satellite  
208 data: methods, challenges, and results. *Remote Sensing of Environment*, **124**, 832–843, ISSN 00344257 (doi:  
209 10.1016/j.rse.2012.06.020)
- 210 Hugonnet R, Brun F, Berthier E, Dehecq A, Mannerfelt ES, Eckert N and Farinotti D (2022) Uncertainty analysis  
211 of digital elevation models by spatial inference from stable terrain. *IEEE Journal of Selected Topics in Applied*  
212 *Earth Observations and Remote Sensing*, 1–17, ISSN 1939-1404, 2151-1535 (doi: 10.1109/JSTARS.2022.3188922)
- 213 Kääb A, Bazilova V, Leclercq PW, Mannerfelt ES and Strozzi T (2023) Global clustering of recent glacier surges  
214 from radar backscatter data, 2017–2022. *Journal of Glaciology*, 1–9, ISSN 0022-1430, 1727-5652 (doi: 10.1017/jog.  
215 2023.35)
- 216 Koch M, Seehaus T, Friedl P and Braun M (2023) Automated Detection of Glacier Surges from Sentinel-1 Surface  
217 Velocity Time Series—An Example from Svalbard. *Remote Sensing*, **15**(6), 1545, ISSN 2072-4292 (doi: 10.3390/  
218 rs15061545)
- 219 Murray T, Dowdeswell JA, Drewry DJ and Frearson I (1998) Geometric evolution and ice dynamics during a surge  
220 of Bakaninbreen, Svalbard. *Journal of Glaciology*, **44**(147), 263–272, ISSN 0022-1430, 1727-5652 (doi: 10.3189/  
221 S0022143000002604)
- 222 Nuth C, Kohler J, König M, von Deschwanden A, Hagen JO, Kääb A, Moholdt G and Pettersson R (2013) Decadal  
223 changes from a multi-temporal glacier inventory of Svalbard. *The Cryosphere*, **7**(5), 1603–1621, ISSN 1994-0424  
224 (doi: 10.5194/tc-7-1603-2013)
- 225 Nuttall AM, Hagen JO and Dowdeswell J (1997) Quiescent-phase changes in velocity and geometry of Finster-  
226 walderebreen, a surge-type glacier in Svalbard. *Annals of Glaciology*, **24**, 249–254, ISSN 0260-3055, 1727-5644 (doi:  
227 10.3189/S0260305500012258)
- 228 Paul F, Piermattei L, Treichler D, Gilbert L, Girod L, Kääb A, Libert L, Nagler T, Strozzi T and Wuite J (2022)  
229 Three different glacier surges at a spot: what satellites observe and what not. *The Cryosphere*, **16**(6), 2505–2526,  
230 ISSN 1994-0424 (doi: 10.5194/tc-16-2505-2022)
- 231 Post A and Mayo LR (1971) Glacier dammed lakes and outburst floods in Alaska. USGS Numbered Series 455, U.S.  
232 Geological Survey (doi: 10.3133/ha455)
- 233 Rouyet L, Karjalainen O, Niittynen P, Aalto J, Luoto M, Lauknes TR, Larsen Y and Hjort J (2021) Environmen-  
234 tal Controls of InSAR-Based Periglacial Ground Dynamics in a Sub-Arctic Landscape. *Journal of Geophysical*  
235 *Research: Earth Surface*, **126**(7), ISSN 2169-9003, 2169-9011 (doi: 10.1029/2021JF006175)

- 236 Sevestre H and Benn DI (2015) Climatic and geometric controls on the global distribution of surge-type glaciers:  
237 implications for a unifying model of surging. *Journal of Glaciology*, **61**(228), 646–662, ISSN 0022-1430, 1727-5652  
238 (doi: 10.3189/2015JoG14J136)
- 239 Sevestre H, Benn DI, Luckman A, Nuth C, Kohler J, Lindbäck K and Pettersson R (2018) Tidewater Glacier Surges  
240 Initiated at the Terminus. *Journal of Geophysical Research: Earth Surface*, **123**(5), 1035–1051, ISSN 21699003  
241 (doi: 10.1029/2017JF004358)
- 242 Shi Y, Liu G, Wang X, Liu Q, Zhang R and Jia H (2019) Assessing the Glacier Boundaries in the Qinghai-Tibetan  
243 Plateau of China by Multi-Temporal Coherence Estimation with Sentinel-1A InSAR. *Remote Sensing*, **11**(4), 392,  
244 ISSN 2072-4292 (doi: 10.3390/rs11040392)
- 245 Sund M and Eiken T (2004) Quiescent-phase dynamics and surge history of a polythermal glacier: Hessbreen,  
246 Svalbard. *Journal of Glaciology*, **50**(171), 547–555, ISSN 0022-1430, 1727-5652 (doi: 10.3189/172756504781829666)
- 247 Sund M, Eiken T, Hagen JO and Kääb A (2009) Svalbard surge dynamics derived from geometric changes. *Annals*  
248 *of Glaciology*, **50**(52), 50–60, ISSN 0260-3055, 1727-5644 (doi: 10.3189/172756409789624265)
- 249 Sund M, Lauknes TR and Eiken T (2014) Surge dynamics in the Nathorstbreen glacier system, Svalbard. *The*  
250 *Cryosphere*, **8**(2), 623–638, ISSN 1994-0424 (doi: 10.5194/tc-8-623-2014)
- 251 Thomas DJ, Robson BA and Racoviteanu A (2023) An integrated deep learning and object-based image analysis  
252 approach for mapping debris-covered glaciers. *Frontiers in Remote Sensing*, **4**, 1161530, ISSN 2673-6187 (doi:  
253 10.3389/frsen.2023.1161530)
- 254 Vallot D, Adinugroho S, Strand R, How P, Pettersson R, Benn DI and Hulton NRJ (2019) Automatic detection of  
255 calving events from time-lapse imagery at Tunabreen, Svalbard. *Geoscientific Instrumentation, Methods and Data*  
256 *Systems*, **8**(1), 113–127, ISSN 2193-0864 (doi: 10.5194/gi-8-113-2019)
- 257 Weydahl D (2001) Analysis of ERS Tandem SAR coherence from glaciers, valleys, and fjord ice on Svalbard. *IEEE*  
258 *Transactions on Geoscience and Remote Sensing*, **39**(9), 2029–2039, ISSN 01962892 (doi: 10.1109/36.951093)